

Determination of metals in saline and biological matrices by axial inductively coupled plasma atomic emission spectrometry using microconcentric nebulization

Machteld De Wit and Ronny Blust*

Department of Biology, University of Antwerp (RUCA), Groenenborgerlaan 171, B-2020 Antwerp, Belgium

An axial inductively coupled plasma atomic emission spectrometer equipped with a commercially available microconcentric nebulizer (MCN) was evaluated for the determination of metals in saline and biological samples. The performance of the MCN was optimized regarding the sample uptake rate and nebulizer pressure in terms of signal intensity and signal-to-background ratio. The effect of increasing salt concentrations was also studied. The results were compared with those obtained with a standard concentric glass nebulizer (CGN) for sample volumes, sensitivity and stability. The MCN was shown to reduce the sample consumption from several milliliters to a few hundred microliters for multi-element analyses. The analytical performance with the MCN was generally poorer than with the CGN, but the magnitude of the effects is element dependent. For the 18 elements studied, the detection limits range from $0.05 \mu\text{g l}^{-1}$ (Mn) to $30.48 \mu\text{g l}^{-1}$ (Ca) for the CGN and from $0.13 \mu\text{g l}^{-1}$ (Mn) to $173.66 \mu\text{g l}^{-1}$ (Na) for the MCN. Increasing the salt concentration decreases both the sensitivity and signal stability obtained with both nebulizers, but the effects are more pronounced for the MCN. The method was further evaluated by analyzing three BCR reference materials: CRM 63 Milk Powder, CRM 185 Bovine Liver and CRM 278 Mussel Tissue. Overall, the results obtained with both nebulizers showed good agreement with the certified values.

Keywords: Axially viewed inductively coupled plasma atomic emission spectrometry; microconcentric nebulizer; concentric glass nebulizer; biological samples; salt effects

The analysis of biological materials by inductively coupled plasma atomic emission spectrometry (ICP-AES) has been a popular application of the emission technique because of its ease of use, its multi-element capability, its high sample throughput, its tolerance to high salt concentrations and the relatively few matrix effects.^{1,2} The ability of axially viewed ICP-AES to achieve low levels of detection has expanded the application field for trace elemental analysis. Detection limits once attainable only with electrothermal atomic absorption spectroscopy (ETAAS) are, at least in some cases, also accessible with axial ICP-AES, providing a dramatic increase in productivity that previously was not possible.^{3,4} As a result, the use of axial ICP-AES is steadily increasing.⁵⁻¹¹ In its standard configuration, an axial ICP spectrometer is equipped with a pneumatic nebulizer for sample introduction. Although pneumatic nebulization is the most commonly used form of sample introduction, these 'standard' concentric or cross-flow nebulizers show important drawbacks: (i) a low transport efficiency (in combination with a spray chamber, typically 1-2%),¹² (ii) the need for relatively large sample volumes (at least 1 ml), (iii) the limitation to liquid samples and (iv) the simultaneous introduction of analyte and matrix into the plasma, giving rise to both spectral and non-spectral interferences.

In many cases, only a limited amount of biological material is available for multi-element analysis with ICP-AES. Dilution to larger volumes, so that a standard nebulizer can be used, often creates detection problems. The use of the ICP as an ionization source for mass spectrometry could solve this problem, but the investment cost is higher than that of ICP-AES, and more expertise is required for ICP-MS. Therefore, many researchers have investigated alternative sample introduction systems, such as electrothermal vaporization,¹³ direct injection nebulization,¹⁴⁻¹⁶ ultrasonic nebulization¹⁷⁻¹⁹ and thermospray nebulization.^{20,21} Application of these alternatives may offer several advantages over standard pneumatic nebulization, but often at the expense of the advantages of the latter system, such as high sample throughput, good stability, instrumental simplicity and low cost.²²

Debrah *et al.*²³ recently coupled a microconcentric nebulizer (MCN) to an ICP-MS system. This microconcentric nebulizer fits easily on to a conventional spray chamber, operates at low flow rates with an efficiency approaching 50% and its price is only slightly higher than that of the standard pneumatic nebulizers. Published applications have focused mainly on the use of a microconcentric nebulizer in combination with ICP-MS.²³⁻²⁵ Considerably reduced sample consumption, good stability, excellent detection limits and comparable or even suppressed matrix interferences were reported. This is in accordance with the MCN commercial promotional literature, which is also based on the combination of a MCN with ICP-MS.

The objectives of this work were to investigate the use of an MCN with axial ICP-AES to determine trace elements in saline and biological samples. The results were compared with those obtained with a conventional concentric pneumatic nebulizer. The stability and sensitivity of the system were determined in different salt matrices, *i.e.*, aqueous standard solutions, 0.9% m/v saline and 3.5% m/v saline in 1% v/v nitric acid. The method was validated by analyzing milk powder, bovine liver and mussel tissue certified reference materials. We are not aware of previous reports of the use of microconcentric nebulization in combination with axial ICP-AES.

EXPERIMENTAL

Instrumentation

A Varian Liberty Series II inductively coupled plasma atomic emission spectrometer (Varian, N. Springvale, Australia) with an axial torch mount was used for all measurements. In its standard configuration, this instrument is equipped with a Varian high flow K style concentric glass nebulizer and a Varian glass cyclonic spray chamber. The microconcentric nebulizer used was a Model MCN-100 (Cetac Technologies Omaha, NE, USA) mounted on a Varian inert Sturman-Masters double-pass cylindrical spray chamber.

Table 1 Axial ICP-AES instrumental operating conditions

	CGN	MCN
Rf power/kW	1	1
Plasma gas flowrate/l min ⁻¹	15	13.5
Auxilliary gas flowrate/l min ⁻¹	1.5	1.5
Nebulizer pressure/kPa	240	300
PMT voltage/V	750	800
Sample uptake rate/ml min ⁻¹	1.6	0.1
Sample delay/s	15	20
Stabilization time/s	30	45
Rinse time/s	30	45
Integration time/s	3	3
No. of replicates	3	3

The optimized instrumental operating conditions for both configurations and the elemental parameters used in this study are summarized in Tables 1 and 2. Background correction was performed simultaneously with each element line. Element wavelengths were selected in order that the detector would not become light saturated owing to high levels of concomitants such as a high content of alkali elements in the biological samples.

Reagents and standards

High-purity water used in preparing reagent and standard solutions was produced by passing Seradest SD-4000 de-ionized water (Seral, VEL, Leuven, Belgium) through a Milli-Q 185 Plus water purification system (Millipore, Bedford, MA, USA). Nitric acid of 1% v/v diluted from high purity 70% v/v HNO₃ (UCB, VEL, Leuven, Belgium) was used as the reference blank throughout. Multi-element standard solutions were prepared from a 1000 mg l⁻¹ ICP multi-element standard solution IV (Merck, Darmstadt, Germany) by dilution with 1% v/v nitric acid. A 1000 mg l⁻¹ stock solution of As in 1% v/v nitric acid was prepared from analytical-reagent grade As₂O₃ (Merck).

The composition of 11 of chemically defined saltwater solution with a salinity of 3.5% m/v was: 23.5 g NaCl, 4.00 g Na₂SO₄, 0.680 g KCl, 0.196 g NaHCO₃, 1.470 g CaCl₂·2H₂O, 10.78 g MgCl₂·6H₂O and 0.026 g H₃BO₃. The medium was prepared by dissolving the seven analytical-reagent grade

products (Merck) in de-ionized water. Solutions of lower salinity were prepared by dilution of the 3.5% m/v solution with de-ionized water and acidified to 1% v/v nitric acid.

Microwave digestion procedure

The following certified reference materials were analysed: CRM 63 Milk Powder, CRM 185 Bovine Liver and CRM 278 Mussel Tissue (Community Bureau of Reference, Geel, Belgium).

Approximately 0.5 g of sample was weighed accurately ($\pm 0.1\%$) in pre-weighed 50 ml polypropylene tubes on an analytical balance (AT261, Mettler, Greifensee, Switzerland) and 2.5 ml of concentrated nitric acid was added before the samples were placed in a microwave oven. The microwave oven was a Samsung (Seoul, South Korea) MF245 with a turntable, rated at 900 W, featuring programmable time, power and temperature settings. To protect the interior of the oven against corrosive acid fumes, the tubes, including three blanks, were loaded into an airtight polycarbonate Bio-Safe carrier box (Nalgene, Nalge, Rochester, NY, USA). After closing, the box was placed in the microwave oven, which was operated for 5 min at 90 W, 5 min at 180 W, 5 min at 270 W and 5 min at 360 W. The turntable was rotated continuously. After being cooled to room temperature, the box was opened under a fume hood and 30 ml of water were added to each sample tube. Before analysis, the samples were diluted 1 + 1 with water to lower the acidity of the sample.

Statistical methods

Data sets were compared using the non-parametric Wilcoxon matched pairs signed ranks test. Standard and standard addition curves were fitted to straight lines by the method of least squares. Measured mean metal concentrations of the reference materials were compared with certified values using a *t*-test. Median values are defined as the value of a variable in an ordered array that has an equal number of items which are higher or lower. The statistical methods used were as described by Sokal and Rohlf.²⁶

Table 2 Axial ICP-AES elemental parameters

Element	Wavelength/ nm	Peak tracking	Order	Background mode
Ag	328.068	0.080	1	Polynomial plotted background*
Al	396.152	0.040	2	Polynomial plotted background*
As	193.696	0.020	4	Polynomial plotted background*
As	188.979	0.080	1	Off-peak background left
Ba	614.172	0.080	1	Polynomial plotted background*
Ca	317.933	0.040	2	Polynomial plotted background*
Cd	228.802	0.027	3	Off-peak background left
Co	228.616	0.027	3	Polynomial plotted background*
Cr	267.716	0.040	2	Polynomial plotted background*
Cu	327.396	0.040	2	Polynomial plotted background*
Fe	259.940	0.040	2	Polynomial plotted background*
K	769.896	0.080	1	Polynomial plotted background*
Mg	279.806	0.030	2	Off-peak background left
Mn	257.610	0.040	2	Polynomial plotted background*
Na	819.482	0.080	1	Polynomial plotted background*
Ni	231.604	0.040	2	Polynomial plotted background*
Pb	220.353	0.027	3	Polynomial plotted background*
Sr	346.446	0.060	1	Polynomial plotted background*
Zn	213.856	0.027	3	Polynomial plotted background*

*In this mode, the system makes use of a slope-estimating algorithm to determine the background correction positions. The algorithm identifies positions around the scan peak where the slope of one side of the peak is less than or equal to the slope of the other side of the peak. This process selects background correction points outside the peak wavelength range. Points around these positions are fitted to a curve which is used to predict the background signal at the analyte wavelength. This is then subtracted from the analyte signal.

RESULTS AND DISCUSSION

Optimization of nebulization conditions

Optimization of the nebulizer conditions was carried out in terms of sample uptake rate and nebulizer pressure to maximize the response, measured as either the absolute signal or the signal-to-background ratio, for both the standard concentric glass nebulizer (CGN) and the microconcentric nebulizer

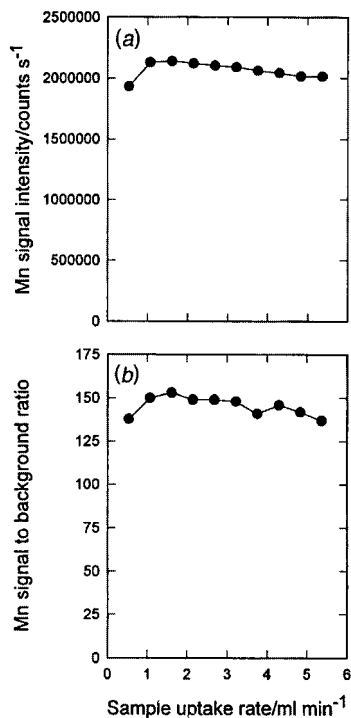


Fig. 1 Mn signal behavior as a function of the sample uptake rate for the concentric glass nebulizer: (a) signal intensity; and (b) signal-to-background ratio.

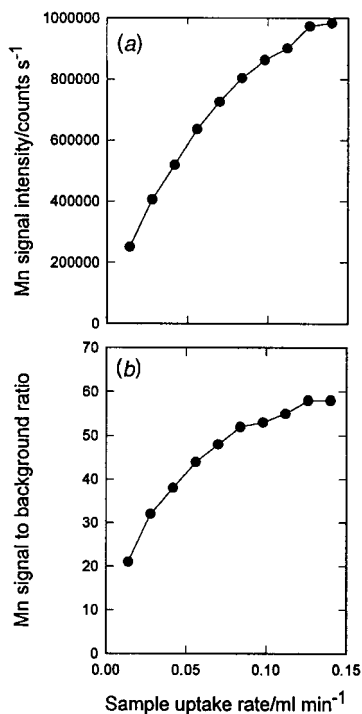


Fig. 2 Mn signal behavior as a function of the sample uptake rate for the microconcentric nebulizer: (a) signal intensity; and (b) signal-to-background ratio.

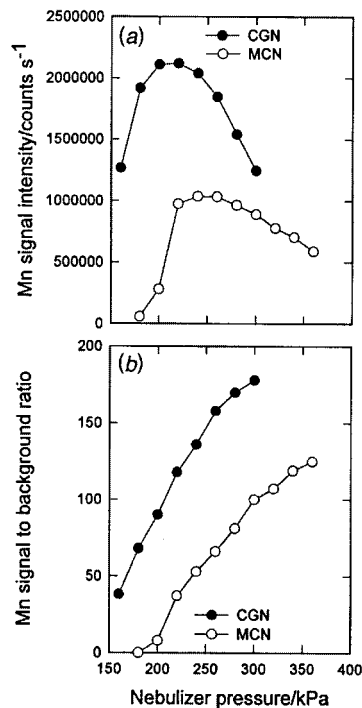


Fig. 3 Mn signal behavior as a function of the nebulizer pressure for the CGN and the MCN: (a) signal intensity; and (b) signal-to-background ratio.

(MCN). Optimization was performed for different elements, generally yielding similar results. Detailed data are presented for Mn, which gave representative results. These results were used to determine the operating conditions which were used for multi-element analysis. An aqueous solution of 1 mg l^{-1} Mn, a concentration well above the background, was used during optimization. The Mn signal behavior is plotted as a function of the sample uptake rate for the standard CGN in Fig. 1 and for the MCN in Fig. 2. It can be observed that for the CGN the signal intensity increases with the sample uptake rate up to about 1 ml min^{-1} , after which the Mn signal intensity decreases gradually. This effect may be the result of several phenomena: first, the increased nebulizer mass transport may be compensated by a lower nebulizer transport efficiency, causing the net mass transport to be roughly constant,²⁷⁻²⁹

Table 3 Comparison of detection limits for the CGN and the MCN

Element	Wavelength/nm	Detection limit/ $\mu\text{g l}^{-1}$		
		CGN	MCN	Ratio
Ag	328.068	0.64	0.69	1.07
Al	396.152	1.92	3.09	1.61
As	193.696	8.15	78.06	9.58
As	188.979	9.30	30.83	3.32
Ba	614.172	0.12	0.56	4.63
Ca	317.933	30.48	2.63	0.09
Cd	228.802	0.28	0.30	1.06
Co	228.616	0.37	1.07	2.87
Cr	267.716	0.30	0.54	1.79
Cu	327.396	0.73	2.89	3.96
Fe	259.940	0.21	0.72	3.43
K	769.896	4.04	26.95	6.66
Mg	279.806	1.66	11.23	6.76
Mn	257.610	0.05	0.13	2.62
Na	819.482	11.96	173.66	14.52
Ni	231.604	0.61	4.03	6.61
Pb	220.353	0.84	8.66	10.29
Sr	346.446	1.59	2.55	1.60
Zn	213.856	0.10	0.63	6.56

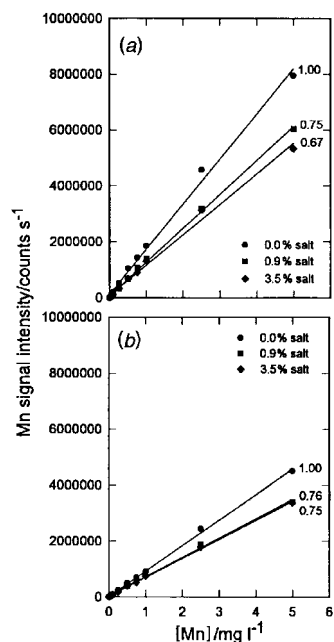


Fig. 4 Effect of increasing salt concentration on Mn signal intensity for (a) the CGN and (b) the MCN. The numbers adjacent to the lines indicate the relative effect of salt on signal intensity.

second, at higher sample uptake rates, the droplet size distribution may become less favorable, causing a larger fraction of the sample to be removed by the spray chamber. A sample uptake rate of 1.6 ml min^{-1} was chosen because at this setting a good signal intensity and signal-to-background ratio were found. For the MCN the signal intensity and signal-to-background ratio increased with increasing sample uptake rate until a plateau was reached. A sample uptake rate of 0.1 ml min^{-1} was chosen because at higher values the signal stability became worse. These results are in agreement with those reported by Vanhaecke *et al.*²⁴ for ICP-MS.

Fig. 3 shows the variation in the Mn signal as function of the nebulizer pressure for both the CGN and the MCN. For the CGN a fairly sharp maximum is observed for signal intensity, whereas the signal-to-background ratio continuously increases. The nebulizer pressure for the CGN was set at 240 kPa since this combines a high signal intensity together

Table 5 Comparison of signal stabilities for the CGN and the MCN in saline solutions (0.0–3.5% salt). Results expressed as RSD for 10 measurements of 1.0 mg l^{-1} standards

Element	Wavelength/nm	RSD (%)					
		CGN			MCN		
		0%	0.9%	3.5%	0%	0.9%	3.5%
Ag	328.068	0.44	0.29	0.43	0.44	0.31	2.11
Al	396.152	0.15	0.59	0.93	1.06	2.07	2.28
As	193.696	0.68	0.59	2.05	0.78	2.08	5.16
As	188.979	0.83	0.69	1.57	1.64	6.36	2.54
Ba	614.172	0.29	0.22	1.03	0.61	0.42	1.02
Ca	317.933	0.29	0.64	0.01	0.33	0.54	0.01
Cd	228.802	0.10	0.40	0.52	1.14	1.05	3.00
Co	228.616	0.26	0.59	0.40	0.04	0.72	5.94
Cr	267.716	0.54	0.68	0.60	0.50	0.57	2.55
Cu	327.396	0.22	0.31	0.51	0.09	1.64	4.61
Fe	259.940	0.38	0.45	0.45	1.04	2.33	0.40
K	769.896	0.30	0.47	0.01	0.46	0.58	2.92
Mg	279.806	0.72	0.43	0.08	0.60	0.88	1.71
Mn	257.610	0.59	0.71	0.61	0.03	0.73	1.40
Na	819.482	0.72	0.36	0.01	8.17	1.14	1.11
Ni	231.604	0.40	0.36	0.31	0.33	1.05	1.92
Pb	220.353	0.21	0.09	0.53	0.92	1.21	2.66
Sr	346.446	1.16	0.20	0.49	1.38	0.88	2.16
Zn	213.856	0.58	0.20	0.46	0.43	1.17	3.21

with a high signal-to-background ratio. For the MCN the maximum signal intensity is shifted towards a higher nebulizer pressure and falls less sharply, whereas the signal-to-background ratio continuously increases. A nebulizer pressure of 300 kPa was chosen for the MCN for the same reason as for the CGN.

It is clear that sample introduction is more efficient for the MCN since a 16-fold decrease in the sample uptake rate results in only a twofold decrease in sensitivity. With the settings given in Tables 1 and 2, determination of the 18 elements listed requires 13.5 ml of sample with the CGN and of 1.3 ml with the MCN.

Detection limits

Detection limits were calculated as three times the standard deviation of 10 successive measurements of the blank. The

Table 4 Comparison of slopes of standard addition curves for the CGN and the MCN in saline solutions (0.0–3.5% salt). Calibration standards ranged from 0–5 mg l^{-1} . Figures in parentheses are relative values

Element	Wavelength/nm	Concentric glass nebulizer/ $10^3 \text{ counts l mg}^{-1} \text{ s}^{-1}$			Microconcentric nebulizer/ $10^3 \text{ counts l mg}^{-1} \text{ s}^{-1}$			Ratio (MCN/CGN)		
		0%	0.9%	3.5%	0%	0.9%	3.5%	0%	0.9%	3.5%
Ag	328.068	398	455 (1.14)	594 (1.49)	207	219 (1.06)	193 (0.93)	0.52	0.48	0.33
Al	396.152	105	128 (1.22)	141 (1.35)	34.0	36.5 (1.07)	35.1 (1.03)	0.32	0.29	0.25
As	193.696	1.59	1.66 (1.04)	1.70 (1.07)	0.725	0.614 (0.85)	0.519 (0.72)	0.45	0.37	0.31
As	188.979	2.88	2.04 (0.71)	1.89 (0.66)	1.34	1.02 (0.76)	0.81 (0.61)	0.47	0.50	0.43
Ba	614.172	2523	1860 (0.74)	1408 (0.56)	783	662 (0.85)	510 (0.65)	0.31	0.36	0.36
Ca	317.933	71.9			46.1			0.64		
Cd	228.802	147	145 (0.99)	174 (1.19)	100	79 (0.79)	73 (0.72)	0.68	0.55	0.42
Co	228.616	74.1	51.4 (0.69)	41.8 (0.56)	40.5	29.8 (0.74)	26.0 (0.64)	0.55	0.58	0.62
Cr	267.716	176	131 (0.74)	117 (0.67)	102	86 (0.84)	72 (0.71)	0.58	0.66	0.62
Cu	327.396	160	159 (0.99)	162 (1.01)	50.8	46.6 (0.92)	40.0 (0.79)	0.32	0.29	0.25
Fe	259.940	330	236 (0.72)	202 (0.61)	167	135 (0.81)	123 (0.74)	0.51	0.57	0.61
K	769.896	52.6			10.7			0.20		
Mg	279.806	29.1			11.5			0.40		
Mn	257.610	1617	1215 (0.75)	1091 (0.67)	911	689 (0.76)	680 (0.75)	0.56	0.57	0.62
Na	819.482	3.48			0.997			0.29		
Ni	231.604	55.0	38.0 (0.69)	29.9 (0.54)	29.7	22.5 (0.76)	20.5 (0.69)	0.54	0.59	0.69
Pb	220.353	13.5	10.0 (0.74)	8.3 (0.61)	7.07	5.53 (0.78)	3.79 (0.54)	0.52	0.55	0.46
Sr	346.446	129	98 (0.76)	89 (0.69)	71.3	65.3 (0.92)	59.5 (0.84)	0.55	0.67	0.67
Zn	213.856	194	165 (0.85)	190 (0.98)	128	90 (0.71)	82 (0.64)	0.66	0.55	0.43

Table 6 Measured concentrations (\pm standard deviation of three replicates) of trace metals in biological reference materials compared with certified values for measurements with the CGN. Values in parentheses are not certified. Significant differences (*t*-test, $p < 0.05$) are identified with asterisks

Element	CRM 63 Milk Powder		CRM 185 Bovine Liver		CRM 278 Mussel Tissue	
	Measured value	Certified value	Measured value	Certified value	Measured value	Certified value
Al/ $\mu\text{g g}^{-1}$					14 \pm 0*	(70)
As/ $\mu\text{g g}^{-1}$			nd [†]	0.024 \pm 0.002	nd	5.9 \pm 0.3
As/ $\mu\text{g g}^{-1}$			nd	0.024 \pm 0.002	nd	5.9 \pm 0.3
Ba/ $\mu\text{g g}^{-1}$					0.5 \pm 0.1	(0.7)
Ca/mg g ⁻¹	12.4 \pm 0.0	12.6 \pm 0.6	0.129 \pm 0.014	(0.131)	1 \pm 0	(1)
Cd/ $\mu\text{g g}^{-1}$	nd	0.0029 \pm 0.0018	0.302 \pm 0.025	0.298 \pm 0.023	0.34 \pm 0.00	0.34 \pm 0.03
Co/ $\mu\text{g g}^{-1}$					0.34 \pm 0.07	(0.34)
Cr/ $\mu\text{g g}^{-1}$			nd	(0.047–0.124)	0.73 \pm 0.04	0.80 \pm 0.07
Cu/ $\mu\text{g g}^{-1}$	0.541 \pm 0.146	0.545 \pm 0.060	183 \pm 15	189 \pm 6	9.6 \pm 0.2	9.6 \pm 0.4
Fe/ $\mu\text{g g}^{-1}$	2.03 \pm 0.27	2.06 \pm 0.50	216 \pm 25	214 \pm 9	127 \pm 8	133 \pm 7
K/mg g ⁻¹	18.0 \pm 0.1	17.8 \pm 1.41	10.8 \pm 0.7	(11.2)	4.6 \pm 0.1	(4.8)
Mg/mg g ⁻¹	1.11 \pm 0.01	1.12 \pm 0.06	0.607 \pm 0.049	(0.634)	1.5 \pm 0.1	(1.4)
Mn/ $\mu\text{g g}^{-1}$	0.429 \pm 0.170*	(0.226)	9.3 \pm 1.6	9.3 \pm 0.3	7.0 \pm 0.0	7.3 \pm 0.3
Na/mg g ⁻¹	4.03 \pm 0.12*	4.57 \pm 0.32	1.3 \pm 0.1*	(2.1)	19 \pm 0	(20)
Ni/ $\mu\text{g g}^{-1}$	nd	(0.011)	1.4 \pm 0.5	(1.4)	1 \pm 0	(1.0)
Pb/ $\mu\text{g g}^{-1}$	nd	0.1045 \pm 0.0117	nd	0.501 \pm 0.038	1.81 \pm 0.1	1.91 \pm 0.07
Sr/ $\mu\text{g g}^{-1}$					14.0 \pm 1.9	(14.5)
Zn/ $\mu\text{g g}^{-1}$	42 \pm 0	(42)	140 \pm 13	142 \pm 5	79 \pm 3	76 \pm 4

[†]nd = Not detectable.

results obtained for both nebulizers are compared in Table 3. The differences in detection limits obtained with the two nebulizers are very much element dependent. For all but one element the detection limits obtained with the MCN are higher than those with the CGN (Wilcoxon's signed ranks test, $p = 0.00170$, $n = 19$). For the 18 elements studied the ratio of the detection limits for the MCN and CGN ranges from 0.09–14.5 with a median value of 3.4.

Salt effects

The effect of salt on the analytical performance was studied by measuring element signal intensity as function of the element concentration in salt matrices, *i.e.*, 0, 0.9, and 3.5% chemically defined saline, with the two nebulizers. For both the CGN and the MCN, the introduction of salt leads to a suppression of

the signal intensity, as shown for Mn in Fig. 4. The result is a decrease in the slope of the linear curve fitted to the data. This is due to the fact that high salt concentrations modify the nebulization efficiency, the plasma ionization conditions and hence the signal intensity.^{30,31} The effects of salt concentration on the slopes of the curves obtained for the different elements, salt concentrations and nebulizers are given in Table 4. The effect can be corrected for by calibration with matrix matched standards or the method of standard additions. Increasing the salt concentration decreases the sensitivity of the analysis for most, but not all, elements. For the CGN the ratio of the slopes measured with and without salt has a median value of 0.752 (minimum 0.691, maximum 1.219) at 0.9% salt and 0.675 (minimum 0.543, maximum 1.493) at 3.5% salt. For the MCN the ratio of the slopes measured with and without salt has a median value of 0.808 (minimum 0.706, maximum 1.073) at

Table 7 Measured concentrations (\pm standard deviation of three replicates) of trace metals in biological reference materials compared with certified values for measurements with the MCN. Values in parentheses are not certified. Significant differences (*t*-test, $p < 0.05$) are identified with asterisks

Element	CRM 63 Milk Powder		CRM 185 Bovine Liver		CRM 278 Mussel Tissue	
	Measured value	Certified value	Measured value	Certified value	Measured value	Certified value
Al/ $\mu\text{g g}^{-1}$					17 \pm 1*	(70)
As/ $\mu\text{g g}^{-1}$			nd [†]	0.024 \pm 0.002	6.1 \pm 0.2	5.9 \pm 0.3
As/ $\mu\text{g g}^{-1}$			nd	0.024 \pm 0.002	nd	5.9 \pm 0.3
Ba/ $\mu\text{g g}^{-1}$					0.5 \pm 0.1	(0.7)
Ca/mg g ⁻¹	11.9 \pm 0.0	12.6 \pm 0.60	0.138 \pm 0.005	(0.131)	1.09 \pm 0.03	(1)
Cd/ $\mu\text{g g}^{-1}$	nd	0.0029 \pm 0.0018	0.282 \pm 0.056	0.298 \pm 0.023	0.35 \pm 0.05	0.34 \pm 0.03
Co/ $\mu\text{g g}^{-1}$					0.31 \pm 0.01	(0.34)
Cr/ $\mu\text{g g}^{-1}$			nd	(0.047–0.124)	0.82 \pm 0.18	0.80 \pm 0.07
Cu/ $\mu\text{g g}^{-1}$	0.555 \pm 0.086	0.545 \pm 0.060	177 \pm 7	189 \pm 6	8.9 \pm 0.2	9.6 \pm 0.4
Fe/ $\mu\text{g g}^{-1}$	1.99 \pm 0.64	2.06 \pm 0.50	209 \pm 5	214 \pm 9	133 \pm 3	133 \pm 7
K/mg g ⁻¹	11.1 \pm 0.4*	17.8 \pm 1.41	6.5 \pm 0.3*	(11.2)	4.4 \pm 0.5	(4.8)
Mg/mg g ⁻¹	1.14 \pm 0.02	1.12 \pm 0.06	0.675 \pm 0.026	(0.634)	1.5 \pm 0.0	(1.4)
Mn/ $\mu\text{g g}^{-1}$	0.204 \pm 0.019	(0.226)	8.9 \pm 0.4	9.3 \pm 0.3	7.9 \pm 0.1*	7.3 \pm 0.3
Na/mg g ⁻¹	4.17 \pm 0.51	4.57 \pm 0.32	1.3 \pm 0.1*	(2.1)	20 \pm 1	(20)
Ni/ $\mu\text{g g}^{-1}$	nd	(0.011)	nd	(1.4)	1.1 \pm 0.0	(1.0)
Pb/ $\mu\text{g g}^{-1}$	nd	0.1045 \pm 0.0117	nd	0.501 \pm 0.038	2.03 \pm 0.37	1.91 \pm 0.07
Sr/ $\mu\text{g g}^{-1}$					14.0 \pm 1.9	(14.5)
Zn/ $\mu\text{g g}^{-1}$	41 \pm 1	(42)	142 \pm 5	142 \pm 5	74 \pm 2	76 \pm 4

[†]nd = Not detectable.

0.9% salt and 0.716 (minimum 0.536, maximum 1.031) at 3.5% salt. Comparing the ratios of the slopes obtained for the different elements with the two nebulizers in the three different salt matrices shows that the absolute sensitivities obtained with the MCN are consistently lower than those obtained with the CGN. The ratio of the slopes measured has a median value of 0.520 (minimum 0.203, maximum 0.682) for the 0% salt solutions, 0.546 (minimum 0.285, maximum 0.666) for the 0.9% salt solutions and 0.430 (minimum 0.247, maximum 0.686) for the 3.5% salt solutions. Wilcoxon's signed ranks test shows that the effect is highly significant for the three groups (0% salt, $p=0.000132$; 0.9% salt, $p=0.000656$; 3.5% salt, $p=0.000656$). Whether the ratio of the slopes increases or decreases with increasing salt concentration depends on the element, but Wilcoxon's signed ranks test shows that there is no general trend (0 and 0.9% salt group, $p=0.733$, $n=15$; and 0 and 3.5% salt groups, $p=0.496$, $n=15$).

The effect of salt concentration on signal stability was measured by determining the relative standard deviation (RSD) for 10 consecutive runs. The results of these measurements are given in Table 5. To evaluate the performance of the two nebulizers, the RSDs obtained for the different elements were compared. The values obtained depend on the element being considered, but generally the signal stability is better for the CGN than the MCN. The differences are not significant for the 0% salt solutions (Wilcoxon's signed ranks test, $p=0.067$, $n=19$), but highly significant for the 0.9% ($p=0.00046$, $n=19$) and 3.5% ($p=0.00033$, $n=19$) salt solutions. Increasing the salt concentration of the solution does not significantly influence the signal stability obtained with the CGN (Wilcoxon's signed ranks tests: 0 and 0.9% salt groups, $p=0.936$, $n=19$ and 0 and 3.5% salt groups, $p=0.355$, $n=19$), but strongly influences the signal stability obtained with the MCN (Wilcoxon's signed ranks tests: 0 and 0.9% salt groups, $p=0.02423$, $n=19$; and 0 and 3.5% salt groups, $p=0.00377$, $n=19$). For As the higher RSD is due to the lowered sensitivity obtained with the MCN for this element so that a concentration of 1 mg l^{-1} is close to the background equivalent concentration. For Na a relatively insensitive line had to be selected in order to be able to measure Na in the very high saline Na environment so that a concentration of 1 mg l^{-1} is close to the background equivalent concentration.

Hence, in solutions of low salt content the signal stabilities are comparable for the two nebulizers, although element-specific differences exist. Increasing the salt concentration decreases the performance of the MCN more than the performance of the CGN.

An important practical observation is that in spite of the small internal diameter, continuous nebulization of solutions containing up to 3.5% salt for several hours does not cause clogging of the capillary of the MCN. Tissue samples, however, that are not completely digested and still contain small particles may cause clogging of the MCN.

Analysis of biological reference materials

The results of the analysis of CRM 63 Milk Powder, CRM 185 Bovine Liver and CRM 278 Mussel Tissue are given in Table 6 for the CGN and in Table 7 for the MCN. As can be seen, good accuracy and precision were obtained for both nebulizers. Except for a few cases, differences in concentrations determined with both set-ups were in good agreement (t -test, $p<0.05$). Hence, the MCN proves a valuable alternative to

the CGN for the determination of metals in saline and biological matrices when the sample volume is limited. The analytical performance decreases to a certain extent, but such effects are only of concern when working close to the detection limit or in high salt matrices.

R.B. is a research associate of the Fund for Scientific Research. This work is part of contract 2012794 with the Fund for Scientific Research, Flanders.

REFERENCES

- Brown, A. A., Halls, D. J., and Taylor, A., *J. Anal. At. Spectrom.*, 1986, **1**, 29R.
- Taylor, A., Branch, S., Crews, H. M., Halls, D. J., Owen, L. M. W., and White, M., *J. Anal. At. Spectrom.*, 1997, **12**, 119R.
- Alavosus, T. J., Murphy, R., and Schatzlein, D., *Am. Lab.*, 1995, **27**, 31.
- Mermert, J. M., and Poussel, E., *Appl. Spectrosc.*, 1995, **49**, 12A.
- Conver, T. S., Yang, J., Koropchak, J. A., Shkolnik, F., and Flajnik-Rivera, C., *Appl. Spectrosc.*, 1997, **51**, 68.
- Ivaldi, J. C., and Tyson, J. F., *Spectrochim. Acta, Part B*, 1995, **50**, 1207.
- Ivaldi, J. C., and Tyson, J. F., *Spectrochim. Acta, Part B*, 1996, **51**, 1443.
- Nakamura, Y., Takahashi, K., Kujirai, O., and Okochi, H., *J. Anal. At. Spectrom.*, 1997, **12**, 349.
- Nakamura, Y., Takahashi, K., Kujirai, O., Okochi, H., and Mcleod, C. W., *J. Anal. At. Spectrom.*, 1994, **9**, 751.
- Dubuisson, C., Poussel, E., and Mermert, J. M., *J. Anal. At. Spectrom.*, 1997, **12**, 281.
- Kato, T., Uehiro, T., Yasuhara, A., and Morita, M., *J. Anal. At. Spectrom.*, 1992, **7**, 15.
- Sharp, B. L., Barnett, N. W., Burrige, J. C., and Ottaway, J. M., *J. Anal. At. Spectrom.*, 1986, **1**, 121R.
- Shen, W.-L., Caruso, J. A., Fricke, F. L., and Satzger, R. D., *J. Anal. At. Spectrom.*, 1990, **45**, 779.
- Wiederin, D. R., Smith, F. G., and Houk, R. S., *Anal. Chem.*, 1991, **63**, 219.
- Powell, M. J., Quan, E. S. K., Boomer, D. W., and Wiederin, D. R., *Anal. Chem.*, 1992, **64**, 2253.
- Shum, S. C. K., and Houk, R. S., *Anal. Chem.*, 1993, **65**, 2972.
- Thompson, J. J., and Houk, R. S., *Anal. Chem.*, 1986, **58**, 2541.
- Montaser, A., Tan, H., Ishii, I., Nam, S.-H., and Cai, M., *Anal. Chem.*, 1991, **63**, 2660.
- Fassel, V. A., and Bear, B. R., *Spectrochim. Acta, Part B*, 1986, **41**, 1089.
- Vanhoe, H., Moens, L., and Dams, R., *J. Anal. At. Spectrom.*, 1994, **9**, 815.
- Koropchak, J., and Winn, D. H., *Appl. Spectrosc.*, 1987, **41**, 1311.
- Browner, R. F., and Boorn, A. W., *Anal. Chem.*, 1984, **56**, 786A.
- Debrah, E., Beres, S. A., Gluodenis, T. J., Thomas, R. J., and Denoyer, E. R., *At. Spectrosc.*, 1995, **16**, 197.
- Vanhaecke, F., Van Holderbeke, M., Moens, L., and Dams, R., *J. Anal. At. Spectrom.*, 1996, **11**, 543.
- Augagneur, S., Médina, B., Szpunar, J., and Lobinski, R., *J. Anal. At. Spectrom.*, 1996, **11**, 713.
- Sokal, R. R., and Rohlf, F. J., in *'Biometry'*, Freeman, San Francisco, 2nd edn., 1981, p. 859.
- Vanhaecke, F., Vandecasteele, C., Vanhoe, H., and Dams, R., *Mikrochim. Acta*, 1992, **108**, 41.
- Long, S. E., and Brown, R. M., *Analyst*, 1986, **111**, 901.
- Browner, R. F., Boorn, A. W., and Smith, D. D., *Anal. Chem.*, 1982, **54**, 1411.
- Olivares, J. A., and Houk, R. S., *Anal. Chem.*, 1986, **58**, 20.
- Grégoire, D. C., *Spectrochim. Acta, Part B*, 1987, **42**, 895.

Paper 8/00253C
Received January 8, 1998
Accepted March 27, 1998